High-resolution quantitative phase-contrast microscopy by digital holography

Christopher J. Mann, Lingfeng Yu, Chun-Min Lo, and Myung K. Kim

Dept. of Physics, University of South Florida, Tampa, FL 33620
mkkim@cas.usf.edu

Abstract: Techniques of digital holography are improved in order to obtain high-resolution, high-fidelity images of quantitative phase-contrast microscopy. In particular, the angular spectrum method of calculating holographic optical field is seen to have significant advantages including tight control of spurious noise components. Holographic phase images are obtained with 0.5 μm diffraction-limited lateral resolution and largely immune from the coherent noise common in other holographic techniques. The phase profile is accurate to about 30 nm of optical thickness. Images of SKOV-3 ovarian cancer cells display intracellular and intranuclear organelles with clarity and quantitative accuracy.

OCIS codes: (090.1760) Computer holography; (090.2880) Holographic interferometry; (180.3170) Interference microscopy

References and links

1. P. Torok and F.J. Kao, *Optical imaging and microscopy* (Springer-Verlag, 2003).
2. A. Barty, K. A. Nugent, D. Paganin and A. Roberts, "Quantitative optical phase microscopy," Opt. Lett. **23**, 817-9 (1998).
3. G. Popescu, L. P. Delflores, J. C. Vaughan, K. Badizadegan, H. Iwai, R. R. Dasari and M. S. Feld, "Fourier phase microscopy for investigation of biological structures and dynamics," Opt. Lett. **29**, 2503-5 (2004).
4. C. G. Rylander, D. Dave, T. Akkin, T. E. Milner, K. R. Diller and A. J. Welch, "Quantitative phase-contrast imaging of cells with phase-sensitive optical coherence microscopy". Opt. Lett. **29**, 1509-11 (2004).
5. U. Schnars and W.P. Jueptner, *Digital Holography* (Springer-Verlag, 2005).
6. E. Cuche, F. Bevilacqua, and C. Depeursinge, "Digital holography for quantitative phase-contrast imaging," Opt. Lett. **24**, 291-3 (1999).
7. L. Xu, X. Peng, J. Miao, and A.K. Asundi, "Studies of digital microscopic holography with applications to microstructure testing", Appl. Opt. **40**, 5046-51 (2001).
8. I. Yamaguchi, J. Kato, S. Ohta, and J. Mizuno, "Image formation in phase-shifting digital holography and applications to microscopy," Appl. Opt. **40**, 6177-86 (2001).
9. Zhang, T. and I. Yamaguchi, "Three-dimensional microscopy with phase-shifting digital holography," Opt. Lett. **23**, 1221 (1998).
10. P. Ferraro, S. De Nicola, A. Finizio, G. Coppola, S. Grilli, C. Magro, and G. Pierattini, "Compensation of the inherent wave front curvature in digital holographic coherent microscopy for quantitative phase-contrast imaging," Appl. Opt. **42**, 1938-46 (2003).
11. M.K. Kim, "Tomographic three-dimensional imaging of a biological specimen using wavelength-scanning digital interference holography," Opt. Express **7**, 305-10 (2000), http://www.opticsexpress.org/abstract.cfm?URI=OPEX-7-9-305.
12. J. Gass, A. Dakoff, and M.K. Kim, "Phase imaging without 2π ambiguity by multiple-wavelength digital holography," Opt. Lett. **28**, 1141-3 (2003).
13. Marquet, B. Rappaz, P.J. Magistretti, E. Cuche, Y. Emery, T. Colomb, and C. Depeursinge, "Digital holographic microscopy: a noninvasive contrast imaging technique allowing quantitative visualization of living cells with subwevelength axial accuracy", Opt. Lett. **30**, 468-70 (2005).
14. J. W. Goodman, *Introduction to Fourier Optics* (McGraw-Hill, 1996).
15. Lingfeng Yu and Myung K Kim, "Wavelength-scanning digital interference holography for tomographic 3D imaging using the angular spectrum method," Opt. Lett. **30**, 2092 (2005).
16. T. M. Kreis, M. Adams and W. P. O. Jueptner, "Methods of digital holography: a comparison," Proc. SPIE **3098**, 224-33 (1997).

#8260 - $15.00 USD Received 25 July 2005; revised 9 September 2005; accepted 9 September 2005

1. Introduction

Many microscopic biological specimens, such as living cells and their intracellular constituents, are mostly transparent, and therefore are problematic for conventional bright-field microscopy. There have been developed a number of techniques for rendering the transparent phase objects visible that have played very important roles in the development of modern biology and medicine[1], and they include the dark field, Zernike phase-contrast, and Nomarski differential interference contrast (DIC) microscopies. In dark field microscopy, only the scattering centers and boundaries contribute to the image signal against a zero background. In the phase contrast microscope, the phase variation is converted into amplitude variation, and in DIC, the interference of two sheared polarization components result in images that have shadow effect and thus give three-dimensional perception of the object. In any of these techniques, the phase to amplitude conversion is nonlinear and there are significant artifacts in the images such as the halo in phase contrast and the disappearance of contrast along the direction perpendicular to shear in DIC. Quantitative phase imaging is not feasible with these techniques.

Quantitative phase imaging is important because it allows the determination of the optical thickness profile of a transparent object with sub-wavelength accuracy. The optical thickness profile depends on the physical thickness as well as the optical index variation, and thus one can extract these information with great accuracy[2]. White-light interference microscopy[3] and optical coherence microscopy[4] have been used to generate quantitative phase image but these require multiple exposure or mechanical scanning. Digital holography[5], an emergent imaging technique, offers an excellent approach for quantitative phase imaging. A hologram that consists of the interference between the object and the reference beams is recorded by a CCD camera and the holographic image is numerically reconstructed inside a computer using the results of diffraction theory. Calculation of the complex optical field allows direct access of both the amplitude and phase information of the optical field[6-8], and by numerical focusing, the images can be obtained at any distance from a single recorded hologram[9]. Digital holography also affords numerous digital processing techniques for manipulating the optical field information in ways that are difficult or impossible in real space processing. For example, optical system aberration can be numerically corrected[10] and multi-wavelength interferometry[11,12] can be accomplished with precise control of the reconstruction wavelengths. Quantitative phase contrast image of neurons has recently been obtained using digital holography[13].

In this paper, we report the results of recent experiments to improve the techniques of digital holography in order to obtain high-resolution, high-fidelity images of quantitative phase-contrast microscopy. We have obtained 0.5 μm diffraction-limited resolution, with the noise level in the phase profile corresponding to about 30 nm of optical thickness. Images of SKOV-3 ovarian cancer cells display intracellular and intranuclear organelles with sufficient clarity and quantitative accuracy for applications in biomedical research. The improvement is achieved in main part by the use of the angular spectrum method[14,15] for diffraction calculation, which has several advantages over more commonly used Fresnel transformation or Huygens convolution method[13]. Spurious noise and interference components can be tightly controlled through the analysis and filtering of the angular spectrum. The reconstruction distance does not have a lower limit and the off-axis angle between the object and reference can be lower than the Fresnel requirement and still be able to cleanly separate out the zero-order background.

2. Experimental

The digital holography experiments are performed using the apparatus depicted in Fig. 1. A miniature pulsed YAG laser (Continuum Minilite) operates at about 2 mJ per Q-switched 10 ns pulse and 532 nm wavelength. The laser output, spatial-filtered and collimated, is split into reference and object beams in an interferometer based on the Mach-Zehnder configuration. The object specimen, mounted on an xyz-translation stage, is placed at a distance *z* from the

#8260 - $15.00 USD Received 25 July 2005; revised 9 September 2005; accepted 9 September 2005

hologram plane *H*, whose magnified image is projected on the CCD camera, as well as the reference beam. A pair of similar microscope objectives, either 20X, 0.4NA or 40x, 0.65NA depending on the desired lateral magnification, are used in the two optical branches to match the curvatures of the two wavefronts. A slight angle is introduced between the object and the reference beams by tilting the beam splitter BS2 for off-axis holography. The camera (Sony DFW-V500) has an array of 640 x 480 pixels on a 4.7 x 3.6 mm^2 active area, with 8-bit gray scale output. A digital delay generator (Stanford Research DG535) triggers both the laser and the camera at a repetition rate of 20 Hz. An IEEE1394 cable connects the camera to the desktop computer, which processes the acquired images and calculates the holographic diffraction using a number of programs based on LabVIEW® and MatLab®.

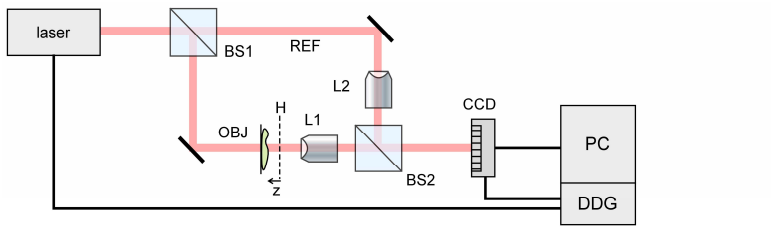

Fig. 1. Apparatus for digital holography experiments. See text for details

There are a number of numerical methods available to calculate the holographic diffraction[6-8,13,15,16]. The most commonly used method has been the Fresnel transformation[6], where the approximation of spherical Huygens wavelet by a parabolic surface allows the calculation of diffraction integral using a single Fourier transform. In the convolution method[8], the diffraction integral is calculated without such approximation using three Fourier transforms through the convolution theorem. On the other hand, the angular spectrum method[15] involves two Fourier transforms, plus simple filtering of the angular spectrum. We have applied all three methods to the reconstruction of the image of a resolution target, as shown in Fig. 2. A 25 x 25 μm^2 area of USAF resolution target is imaged containing the group 7 element 6 using 452 x 452 pixels. Figure 2(a) is the holographic interference pattern recorded by the CCD camera, and its Fourier transform in Fig. 2(b) is the angular spectrum. It contains three main peaks that correspond to the spectra of the zero-order and the two twin-images. One of these peaks – the highlighted rectangular area – is selected, a propagation phase factor (z = 7 μm) is multiplied, and finally inverse-Fourier transformed to obtain the amplitude image in Fig. 2(c) and the phase image in Fig. 2(d). The individual bars are 2.2 μm wide, which are clearly resolved and consistent with diffraction-limited resolution of 0.5 μm for 0.65 NA lens. The resolution target is a positive mask with opaque chrome film pattern on transparent glass plate, used in transmission. From the analysis of the phase map, the phase step of the metal strip is $\sim 52°$. The physical thickness of film is given by $d = \lambda(\Delta\varphi / 2\pi)/(n - n_0)$, where λ is the wavelength, $\Delta\varphi$ is the phase step, and $(n - n_0)$ is the index difference between the film and air. Using a known estimate of the film thickness of 50 nm, the optical index (real part) of the metal film is ~2.5. The noise level of the flat area is $\sim 10°$, which corresponds to glass thickness variation of ~30 nm. (On the film-coated bar areas, the lack of light causes larger uncertainty in phase.) The phase map is rendered in pseudo-colored 3D perspective in Fig. 2(i). Especially notable in the phase map is the lack of the coherent noise conspicuous in the amplitude image and prevalent in most other holographic imaging methods. The amplitude and phase images obtained from the Huygens convolution method are shown in Fig. 2(e) and 2(f), as well as those obtained from the Fresnel method in Fig. 2(g) and 2(h). The main reason for the obvious degradation of these image is the insufficient off-axis angle to separate out the zero-order component. The effect is most detrimental in the Fresnel images, where part of the holographic image is buried in the zero-order background, and its phase image is completely scrambled. The effect shows up as the

#8260 - $15.00 USD Received 25 July 2005; revised 9 September 2005; accepted 9 September 2005

spurious interference patterns in the convolution images. While the minimum off-axis angle must be strictly satisfied in order to avoid the zero-order intrusion in Fresnel or convolution methods, the control and removal of zero-order component is straightforward and flexible in the angular spectrum method. Another potential problem is that the Fresnel and convolution methods require minimum hologram distance to avoid aliasing, whereas the angular spectrum method does not have such minimum and the image can be calculated even at zero distance[15]. The minimum distance is given by $z_{min} = a^2 / N\lambda$ where a is the size of the hologram and N is the number of pixels. For the particular example shown here the minimum distance happens to be 2.6 μm and therefore is not an issue, but the images shown below in Fig. 4 are obtained at z = 5 μm < z_{min} = 18 μm, and the Fresnel or convolution methods would not have worked.

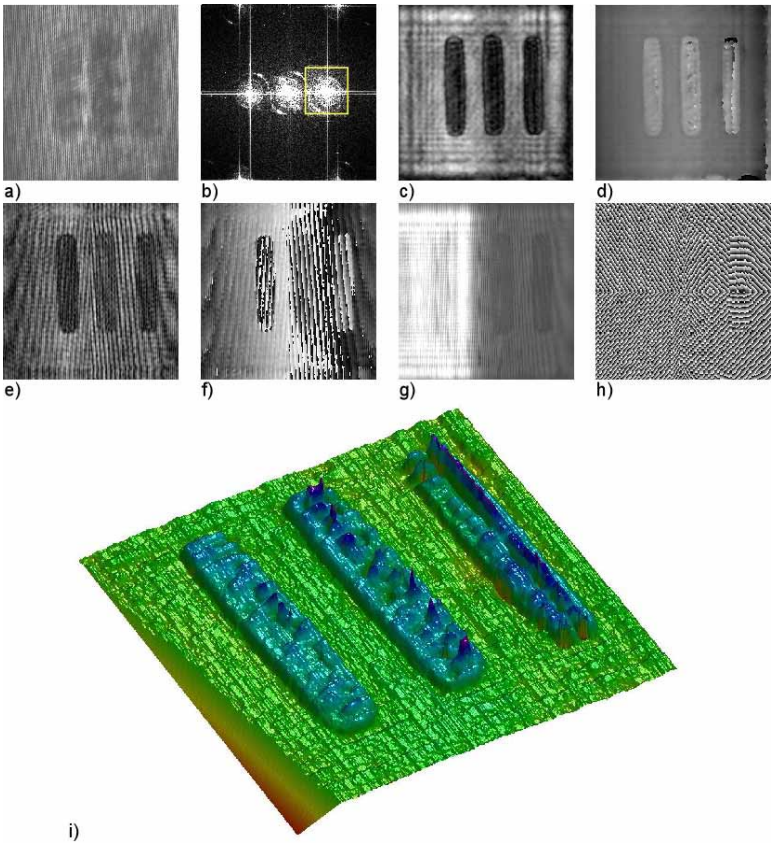

Fig. 2. Holography of a resolution target. The image area is 25 x 25 μm^2 (452 x 452 pixels) and the image is at z = 7 μm from the hologram: (a) hologram; (b) angular spectrum; (c) amplitude and (d) phase images by angular spectrum method; (e) amplitude and (f) phase images by Huygens convolution method; (g) amplitude and (h) phase images by Fresnel transform method; (i) 3D pseudocolor rendering of (d). The individual bars are 2.2 μm wide.

#8260 - $15.00 USD Received 25 July 2005; revised 9 September 2005; accepted 9 September 2005

3. Results

We present two examples of quantitative phase-contrast microscopy studies by angular spectrum digital holography. Figures 3 and 4 show images of SKOV-3 ovarian cancer cells: confluent group of cells in Fig. 3 and two isolated cells in Fig. 4. In each of the two cases, the panels display (a) Zernike phase contrast image (of similar but different portions of the sample than the holography images), (b) holographic amplitude and (c) phase images, and (d) phase image unwrapped by a software algorithm. Pseudocolor 3D rendering of (d) is shown in (e). The image size is 60 x 60 μm^2 with 404 x 404 pixels. In Fig. 3, we see the phenomenon of cuboidal cells connecting together into an epithelial sheet and producing the grooves between cells. A gap in the confluence is also accurately imaged in Fig. 3(e), except for a few spikes due to a defect in the phase-unwrapping algorithm. Figure 4 is a particularly unambiguous demonstration of the level of image resolution and fidelity that can be obtained by the present technique, displaying the nuclear membranes and chromosomes. The overall height of the cell is calculated to be about 2.8 μm, with the assumption of the average index of the cell to be 1.375. Thickness of the lamelipodium around the edge of the cell is determined to be about 320 nm. The noise level in the substrate area is 60 nm, which may be partly due to the residues from fixing of the cells. From this we infer that the corrugated texture of cellular surfaces in Fig. 3(e) is not likely to be noise or artifact of holographic process. Such texture is evident in the Zernike phase contrast image of Fig. 3(a) and is known to exist in such confluent cells. The depth of the texture is estimated to be about 120 nm.

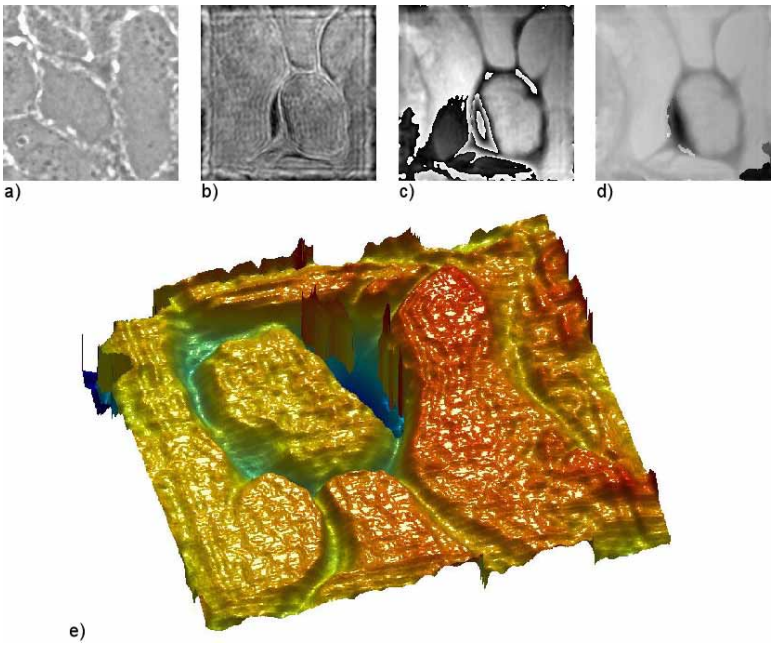

Fig. 3. Holography of confluent SKOV-3 ovarian cancer cells. The image area is 60 x 60 μm^2 (404 x 404 pixels) and the image is at z = 10 μm from the hologram: (a) Zernike phase contrast image; (b) holographic amplitude and (c) phase images; (d) unwrapped phase image; (e) 3D pseudocolor rendering of (d).

#8260 - $15.00 USD Received 25 July 2005; revised 9 September 2005; accepted 9 September 2005

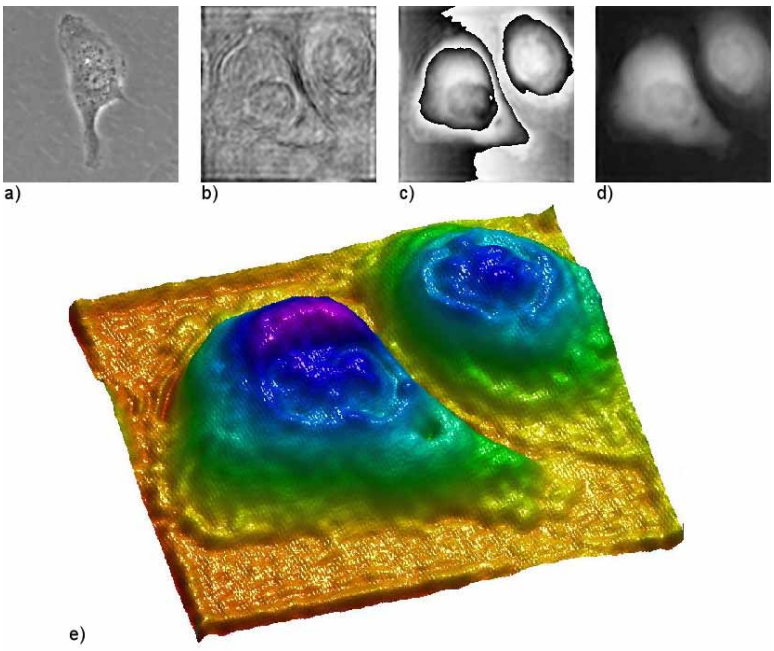

Fig. 4. Holography of non-confluent SKOV-3 cells. The image area is 60 x 60 μm^2 (404 x 404 pixels) and the image is at z = 5 μm from the hologram: (a) Zernike phase contrast image; (b) holographic amplitude and (c) phase images; (d) unwrapped phase image; (e) 3D pseudocolor rendering of (d).

4. Conclusions

To summarize, we have improved techniques of digital holography to obtain high-resolution high-fidelity quantitative phase-contrast images of cells. The use of angular spectrum method is seen to solve some of the significant problems that have prevented wider use of digital holography in biomedical imaging applications. The level of resolution and details in these images clearly exceeds currently available techniques in phase-contrast optical microscopy and provides a new modality for imaging morphology of cellular, intracellular and intranuclear structures that is not currently available with non-invasive optical methods.

This work is supported in part by the National Science Foundation.

#8260 - $15.00 USD Received 25 July 2005; revised 9 September 2005; accepted 9 September 2005